



# Spatial and temporal representativeness of point measurements for nitrogen dioxide pollution levels in cities

Ying Zhu<sup>1,2</sup>, Jia Chen<sup>2</sup>, Xiao Bi<sup>2</sup>, Gerrit Kuhlmann<sup>3</sup>, Ka Lok Chan<sup>4</sup>, Florian Dietrich<sup>2</sup>, Dominik Brunner<sup>3</sup>, Sheng Ye<sup>1</sup>, and Mark Wenig<sup>1</sup>

<sup>1</sup>Meteorological Institute, Ludwig-Maximilians-Universität München, Munich, Germany

<sup>2</sup>TUM Department of Electrical and Computer Engineering, Technische Universität München, Munich, Germany

<sup>3</sup>Empa, Swiss Federal Laboratories for Materials Science and Technology, Überlandstrasse 129, Dübendorf, Switzerland

<sup>4</sup>Remote Sensing Technology Institute (IMF), German Aerospace Center (DLR), Oberpfaffenhofen, Germany

**Correspondence:** Ying Zhu (ying.zhu@physik.uni-muenchen.de), Mark Wenig (mark.wenig@lmu.de), and Jia Chen (jia.chen@tum.de)

Received: 26 December 2019 – Discussion started: 9 March 2020

Revised: 24 July 2020 – Accepted: 24 August 2020 – Published: 10 November 2020

**Abstract.** In many cities around the world the overall air quality is improving, but at the same time nitrogen dioxide (NO<sub>2</sub>) trends show stagnating values and in many cases could not be reduced below air quality standards recommended by the World Health Organization (WHO). Many large cities have built monitoring stations to continuously measure different air pollutants. While most stations follow defined rules in terms of measurement height and distance to traffic emissions, the question remains of how representative are those point measurements for the city-wide air quality. The question of the spatial coverage of a point measurement is important because it defines the area of influence and coverage of monitoring networks, determines how to assimilate monitoring data into model simulations or compare to satellite data with a coarser resolution, and is essential to assess the impact of the acquired data on public health.

In order to answer this question, we combined different measurement data sets consisting of path-averaging remote sensing data and in situ point measurements in stationary and mobile setups from a measurement campaign that took place in Munich, Germany, in June and July 2016. We developed an algorithm to strip temporal from spatial patterns in order to construct a consistent NO<sub>2</sub> pollution map for Munich. Continuous long-path differential optical absorption spectroscopy (LP DOAS) measurements were complemented with mobile cavity-enhanced (CE) DOAS, chemiluminescence (CL) and cavity attenuated phase shift (CAPS) instruments and were compared to monitoring stations and

satellite data. In order to generate a consistent composite map, the LP DOAS diurnal cycle has been used to normalize for the time of the day dependency of the source patterns, so that spatial and temporal patterns can be analyzed separately. The resulting concentration map visualizes pollution hot spots at traffic junctions and tunnel exits in Munich, providing insights into the strong spatial variations. On the other hand, this database is beneficial to the urban planning and the design of control measures of environment pollution. Directly comparing on-street mobile measurements in the vicinity of monitoring stations resulted in a difference of 48 %. For the extrapolation of the monitoring station data to street level, we determined the influence of the measuring height and distance to the street. We found that a measuring height of 4 m, at which the Munich monitoring stations measure, results in 16 % lower average concentrations than a measuring height of 1.5 m, which is the height of the inlet of our mobile measurements and a typical pedestrian breathing height. The horizontal distance of most stations to the center of the street of about 6 m also results in an average reduction of 13 % compared to street level concentration. A difference of 21 % in the NO<sub>2</sub> concentrations remained, which could be an indication that city-wide measurements are needed for capturing the full range and variability of concentrations for assessing pollutant exposure and air quality in cities.

## 1 Introduction

Many former studies (Huang et al., 2014; Dunlea et al., 2007; Jang and Kamens, 2001) have been pointed out that NO<sub>2</sub> is an important composition in the process of both tropospheric and stratospheric chemistry. It is one of the major pollution products from combustion processes. Catalytic formation of tropospheric ozone (O<sub>3</sub>) and the formation of secondary aerosols that cause acid rain, all of which involve its participation. Elevated concentration of atmospheric NO<sub>2</sub> is acknowledged to be noxious to human beings' health. In urban environments, exhaust emissions are one of the primary sources of air pollution, particularly NO<sub>x</sub> (= NO + NO<sub>2</sub>). Nitrogen monoxide (NO) accounts for the majority of direct traffic emissions, which is subsequently oxidized to form NO<sub>2</sub> although some NO<sub>2</sub> is emitted directly (Ban-Weiss et al., 2008; Henderson et al., 2007; Kirchstetter et al., 1999). NO<sub>2</sub> levels are often strongly correlated with many other toxic air pollutants (Massman, 1998; Yoo et al., 2014; Xie et al., 2015). Its concentration can be easily and precisely measured, which is helpful in assessing general air quality. Since it is a short-lived compound gas from numerous different sources, its concentrations can vary strongly, both in space and time.

According to the 2017 European Environment Agency report (EEA, 2017), some NO<sub>2</sub> concentrations measured at air quality monitoring stations are above the World Health Organization (WHO) Air Quality Guideline (AQG) values of 200 µg m<sup>-3</sup> (hourly) and 40 µg m<sup>-3</sup> (annually). A total of 10.5% of the stations across European cities exceeded the annual limits, including several German cities. None of the exceedances were observed at rural background stations but instead in urban or suburban stations. More specifically, 89% of the exceeded values were observed at traffic stations. The 2016 air quality report by the German Environment Agency (Umweltbundesamt) (UBA, 2017) also pointed out that the air pollution in urban conurbations was primarily affected by traffic. In the 2015 technical report by the Bavarian environment agency (Landesamt für Umwelt, LfU) (LfU, 2015), the on-road NO<sub>2</sub> concentration limits were exceeded in most Bavarian cities from 2000 to 2014. In particular, the annual NO<sub>2</sub> level in Munich measured at Landshuter Allee station was more than twice the annual NO<sub>2</sub> limit value of the WHO AQG of 40 µg m<sup>-3</sup>.

With a growing focus on air pollution in the public attention, stationary monitoring networks have been established all over the world. Related regulations also have been certified. For example, in Europe, the European directive 2008/50/EC lists a number of criteria for microscale positioning of air quality measurements (Annex III section C). Monitoring stations in the EU continuously measure different pollutants, and while most stations follow the defined rules in terms of measurement height and distance to traffic emissions, the question remains of how representative are those point measurements for the city-wide air quality. Ac-

ording to a study of the spatial distribution of NO<sub>2</sub> in Hong Kong (Zhu et al., 2018), large differences between mobile measurements around the city and seven local monitoring stations were observed. In order to determine the representativeness of air quality monitoring stations, different measurement methods have to be combined. Most monitoring stations utilize the chemiluminescence (CL) technique for NO<sub>x</sub> measurements. Thereby the NO<sub>2</sub> concentration is determined indirectly by calculating the difference between NO<sub>x</sub> and NO concentrations. The concentration of oxidized odd-Nitrogen species (NO<sub>y</sub>) is inevitably included as a small measurement error. Nevertheless, the CL technique has a good detection sensitivity that is given by its low background signal. This is because for initiating the fluorescence no light source is required (Dunlea et al., 2007). In this study, we compared our CL and cavity-enhanced DOAS (CE DOAS) data to the local air quality stations and studied the diffusion rate of NO<sub>2</sub> in both vertical and horizontal directions from one of the stations.

For our study we utilized a combination of a long-path DOAS (LP DOAS) instrument and a CE DOAS, as well as a cavity attenuated phase shift spectroscopy (CAPS) instrument to determine the spatiotemporal variability of NO<sub>2</sub> concentrations in the central area of Munich. CE DOAS is a spectroscopic measurement technique that uses an optical resonator to fold the absorption path into a resonator (Zhu et al., 2018; Min et al., 2016; Thalman and Volkamer, 2010; Platt et al., 2009; Washenfelder et al., 2008; Venables et al., 2006; Langridge et al., 2006). CAPS (Herbelin et al., 1980) is a spectroscopic detection technology, generally referred to as cavity-enhanced optical absorption, which has also been applied for the detection of atmospheric pollutants in many studies (Xie et al., 2019; Kundu et al., 2019; Ge et al., 2013; Kebabian et al., 2005a, 2008). The advantage of CE DOAS and CAPS is the fact that they are not sensitive to other reactive nitrogen oxides in the atmosphere like some other in situ NO<sub>2</sub> monitoring techniques. They are both characterized by a compact setup and have no sensitivity loss during the operation. For mobile measurements a fast sampling rate is necessary, and the high accuracy of the instruments allowed a sampling rate of 2 s. Similar instrument setups have been used in many on-road studies of vehicles emissions (Zhu et al., 2018; Chan et al., 2017; Rakowska et al., 2014; Ning et al., 2012; Uhrner et al., 2007; Vogt et al., 2003).

For our study we conducted on-road measurements of NO<sub>2</sub> concentrations in June and July 2016 in order to investigate street level air quality and locate emission hot spot areas. Additionally, LP DOAS measurements were conducted to observe the temporal variability of ambient NO<sub>2</sub> in Munich. A measurement system consisting of several DOAS instruments was continuously operational for over 2 years (see Sect. 2). The algorithm that combines the mobile and stationary measurement data is described in Sect. 3.1.1. The resulting on-road NO<sub>2</sub> spatial patterns are presented in Sect. 3.1.2. The CE DOAS and CL were set up next to the Bavarian LfU

local air quality station to measure the horizontal and vertical NO<sub>2</sub> distributions, and the results are shown in Sect. 3.2. NO<sub>2</sub> data from the Ozone Monitoring Instrument (OMI) on board the NASA Aura satellite were used to verify how the LP DOAS measurements compare to the much larger OMI ground pixels covering a larger fraction of the city in order to find out whether the LP DOAS measurements are representative for the whole city. Detailed analysis is provided in the Supplement.

## 2 Methodology

This study combines different measurement methods such as mobile, stationary and satellite measurements to answer the question of how representative sparse point measurements are to determine the air quality of a city. Furthermore, we want to find out what kind of measurement approach is needed to determine the overall air quality in a city. The Munich three-dimensional DOAS measuring system combines three different types of DOAS instruments, specifically, CE DOAS and LP DOAS. The measurement system is installed on the roof of the building of the Meteorological Institute Munich (MIM) at the Ludwig Maximilians University (LMU) in the center of Munich. The three LP DOAS instruments scan retroreflector arrays in different directions and distances, capturing the horizontal variations at the rooftop level. A CE DOAS is used to determine the NO<sub>2</sub> variability on the ground. The LP DOAS instruments run continuously, whereas the CE DOAS is used at different times of the year/week/day under varying meteorological conditions to determine street level NO<sub>2</sub> distributions.

### 2.1 Mobile measurements

A CE DOAS and a CAPS instruments in two vehicles were used for on-street sampling of traffic emissions. The sampling inlets were located at the front right window of each vehicle at 1.5 m height. For measurements in Munich's city park (English Garden), we used a bike trailer. The measurements were performed on two days in March, three days in May, five days in June and six days in July 2016 to cover a large part of the urban area in Munich. Table 1 shows the dates, measurement times and number of measurements for all measurement days. The sample resolutions of the CE DOAS and the CAPS were both adjusted to 2 s during the mobile measurements. The measurements were performed on varying routes during daytime to cover the entire city center area. All measurements were spatially averaged to a high-resolution grid of 20 m × 20 m. This resolution has been chosen according to an average driving speed of 40–50 km h<sup>-1</sup> and the measurement sampling time of 2 s, so that at least one measurement value per drive-by falls into each grid box. All measurements from different drives and different days are averaged for each grid cell after diurnal cycle normalization.

The CE DOAS is composed of an air sampling system, an optical resonator with two highly reflective mirrors, a blue LED light source and a spectrometer (Platt et al., 2009). For the spectral retrieval in the wavelength range 435.6 to 455.1 nm, we used DOASIS (Kraus, 2005). The NO<sub>2</sub> reference absorption cross is from Vandaele et al. (2002), O<sub>4</sub> from Hermans et al. (1999), H<sub>2</sub>O from Rothman et al. (2003) and CHOCHO (glyoxal) from Volkamer et al. (2005).

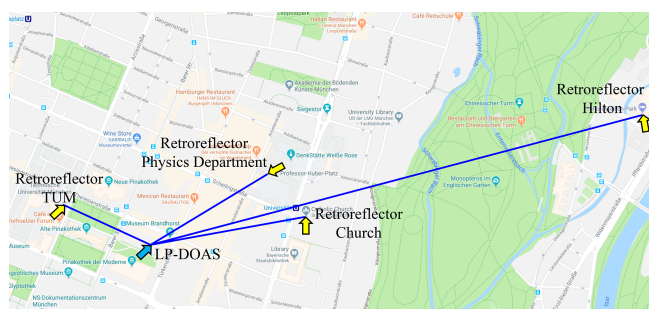
The CAPS measurement technique is closely related to cavity ring-down laser absorption spectroscopy (CRDS), which determines the concentration of trace gases from the decay rate of the light source in the optical resonator (Ball and Jones, 2003; Brown et al., 2002; Berden et al., 2000; Engeln et al., 1996). CRDS is a laser-based system, while CAPS uses an incoherent light source (a blue LED) that is well matched to the NO<sub>2</sub> absorption band. The CAPS NO<sub>2</sub> system mainly consists of a blue LED, a measurement chamber with two highly reflective mirrors centered at 450 nm and a vacuum photodiode detector. It estimates the NO<sub>2</sub> concentration by directly measuring the optical absorption of NO<sub>2</sub> at the 450 nm wavelength within the electromagnetic spectrum. The light appears as a distorted waveform after passing through two mirrors and the measurement cell, which is characterized by a phase shift that is determined by demodulation techniques in comparison to the initial LED light modulation. The phase shift is proportional to the absorbance of the light by the presence of NO<sub>2</sub>. The concentration of NO<sub>2</sub> can be derived by measuring the amount of the phase shift. The detailed principles of the CAPS system are demonstrated in Kebedian et al. (2005b, 2008).

### 2.2 Long-path (LP) DOAS observations

Three LP DOAS instruments were installed on the roof of the MIM. The measurement setups are displayed in Fig. 1. The measurement system started operation in December 2015 with a total absorption path of 3828 m across the English Garden to a retroreflector array located on the rooftop of the Hilton hotel building at ~48 m height. In January 2017 another absorption path of 1142 m was installed covering three blocks around the university area to a retroreflector at the St. Ludwig church in Munich at ~40 m above ground. Since July 2015 a retroreflector has also been installed at the roof of the N5 building of the Technical University of Munich (TUM) at ~28 m height, allowing an absorption path of 828 m. From July 2016 to August 2017 a path of 816 m to the roof of the building of the physics department of LMU at ~24 m height was operational as well. For the long-term average diurnal cycle calculation described in Sect. 3.1.1 all available data from all measurement paths were used. LP DOAS measurements of light paths towards to the Hilton hotel, TUM and the LMU physics department were used to normalize the mobile measurements regarding the diurnal cycle. The measurement paths cover the university campus, the public park, residential areas and areas with heavy traffic.

**Table 1.** Overview of the measurement days, time and number of measurements.

Measurement date (yyyy.mm.dd)	Measurement time (hours)	Number of measurements	Measurement date (yyyy.mm.dd)	Measurement time (hours)	Number of measurements
2016.03.21	3.84	5313	2016.06.16	5.48	7586
2016.03.22	1.82	2523	2016.06.17	2.75	3804
2016.05.09	2.29	3172	2016.07.01	2.86	3955
2016.05.10	3.62	5019	2016.07.06	6.24	17 292
2016.05.11	4.55	6295	2016.07.07	10.29	28 489
2016.06.06	3.38	4674	2016.07.08	5.22	14 466
2016.06.07	4.66	6454	2016.07.11	5.1	14 123
2016.06.13	4.25	5882	2016.07.13	2.48	2976
			Total	64.8	126440

**Figure 1.** Map of Munich city center and four optical paths of three LP DOAS instruments. Map data © Google Maps.

The instrumental background was corrected by subtracting the LED reference spectra, including dark current, offset and background, from each measured spectrum.

A measurement sequence starts by taking a LED reference spectra using a shortcut system consisting of a diffuser plate in front of the y fiber and an exposure time of 10 s. Then a shutter is used to block the LED for measuring the atmospheric background spectrum for 1 s. Afterwards, the atmospheric spectrum with a maximum of 10 scans is taken. Each scan of a spectrum has a peak intensity of about 60%–80% saturation of the detector and typically requires 60–1000 ms, depending on the visibility and instrument setup. The total sampling time (the product of the number of scans and exposure time for each scan) was limited to 60 s. A full measurement sequence took between 30 and 90 s, depending on visibility conditions.

### 2.3 Local air quality monitoring network

The Bavarian LfU is operating five monitoring stations: three roadside stations at Landshuter Allee, Stachus and Lothstraße (locations of the three stations are also presented in Fig. 4c), and two ambient stations in Allach and Johanneskirchen. In these stations the air pollutants NO, NO<sub>2</sub>, CO, O<sub>3</sub>, PM<sub>2.5</sub>, and PM<sub>10</sub> and in addition meteorological param-

eters such as relative humidity and temperature are measured. In this study we concentrated on the NO and NO<sub>2</sub> concentrations that are continuously monitored using an in situ CL NO<sub>x</sub> analyzer (HORIBA APNA-370) (LfU, 2019).

## 3 Results and discussion

### 3.1 NO<sub>2</sub> concentration maps constructed using mobile measurements

The mobile measurement data can be used to create a map showing the city-wide distribution of air quality using NO<sub>2</sub> concentrations as a general indicator (Fig. 4). As a first test, we compared the averaged measurement values within a 10 km radius around the three governmental monitoring stations at Landshuter Allee, Lothstraße, and Stachus and obtained an averaged concentration of 93 µg m<sup>-3</sup> for the mobile measurements and 48 µg m<sup>-3</sup> for the three stations for the campaign days in June and July 2016. The large difference can be explained by looking at the criteria for the location of monitoring sites set by the European Union: the recommended measurement height is between 1.5 and 4 m; maximum distance to the street is 10 m and at a minimum distance to the next crossroad of 25 m (Commission, 2008). Most monitoring stations have the inlet positioned at 4 m height. The mobile measurement data, however, include the significantly increased concentrations at crossroads, tunnel exits and other pollution hot spots. In addition, the height of the measurement inlets differs by 2.5 m between the mobile measurements and the governmental monitoring stations, which also influences the comparison. In order to determine how representative point measurements are for the city-wide air quality, we analyzed the correlation between point measurements and the distribution captured by mobile measurements, between point and path-averaging measurements, as well as between path-averaging and satellite measurements. Since the spatial distribution can not be captured instantaneously, an algorithm to normalize for the diurnal variation is needed in order to create a consistent map representing only the spa-

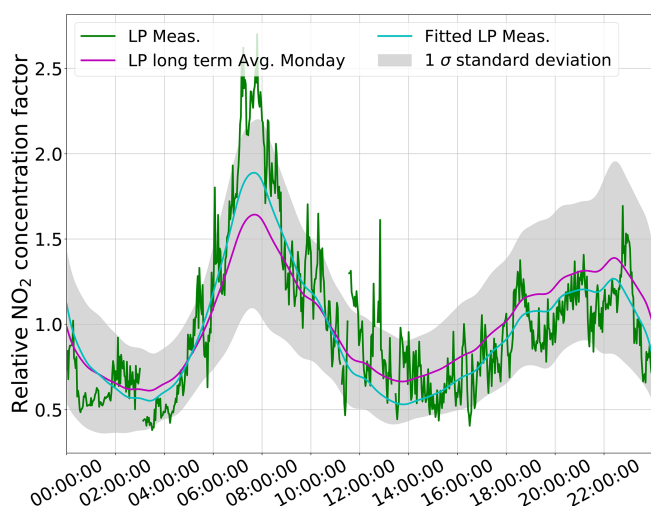


**Figure 2.** Normalization curve used to correct mobile measurement data. The purple curve is the long-term average diurnal pattern for the day of the week of the measurement day (Monday in this example), which is fitted (scaling with the linearly time dependent factor and offset) to the measurement data of 13 June 2016 shown in green, excluding the data outside of the  $2\sigma$  area shown in gray. The resulting cyan curve is used to remove the diurnal dependency of the mobile measurements data.

tial variability of daily average concentrations instead of temporal influences.

### 3.1.1 Normalization of the diurnal cycle

As a mobile survey cannot capture the concentrations at different locations simultaneously, and the  $\text{NO}_2$  measurements are naturally influenced by daily variations such as changing boundary layer height or the diurnal cycle of the traffic amount, we use an algorithm to separate temporal and spatial patterns in the data set.

First, the algorithm normalizes the long time series of LP DOAS measurements of atmospheric  $\text{NO}_2$  by dividing through the daily average  $\text{NO}_2$  concentration of the same day. The mean concentration curves for each day of the week over a period of 2.5 years are calculated in order to obtain a relative diurnal  $\text{NO}_2$  variation pattern (purple curve in Fig. 2). The normalized averaged diurnal  $\text{NO}_2$  curve of the corresponding weekday is fitted (using an offset and a scaling with a linearly time dependent factor) to the normalized LP DOAS measurement of the corresponding day, coinciding with the mobile measurements. In order to remove the influence of outliers,  $\text{NO}_2$  values outside of  $2\sigma$  variation of the fitted curve are disregarded (cyan curve). Fig. 2 shows the fitting process for the normalization curve for one day of the measurement campaign. The other days show very similar characteristics with a significant peak in the morning and evening rush hours. Dividing the mobile measurement data

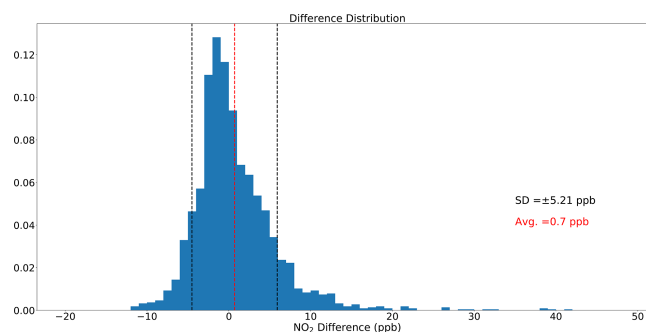


**Figure 3.** The distribution of the differences in between the inferred daily average concentrations and 24 h average concentrations measured by LfU stations. Bin width is 1 ppb. Evaluated stations including Allach, Johanneskirchen and Lothstraße.

by the curve data removes the diurnal dependencies and allows focusing on spatial pattern.

The corresponding stationary measurements from three LfU stations on mobile measurement days were used to evaluate the accuracy of the normalization algorithm. The inferred daily average concentration for each stationary measurement was retrieved based on the fitted LP DOAS normalization curve and then compared with the corresponding 24 h average concentration measured by the same station. The distribution of the concentration differences is shown in Fig. 3. The averaged difference is 0.7 ppb with  $1\sigma$  uncertainty of 5.21 ppb. The inferred daily averages compared to the actual average concentrations at the stations Landshuter Allee and Stachus differ more because due to frequent traffic jams and stop-and-go traffic they show a different diurnal cycle. Overall, the normalization algorithm effectively separated the temporal and spatial influence for most mobile measurement locations.

### 3.1.2 Spatial distribution of $\text{NO}_2$ in the city of Munich

The measured concentrations during the campaign were spatially averaged to a high-resolution grid of  $20\text{ m} \times 20\text{ m}$  (Fig. 4a). Most of these measurements are distributed on major roads, including city, urban ring road, suburbs, rural areas and highways. Relatively high  $\text{NO}_2$  pollution could be observed on motorways and busy urban roads. A difference between main roads and adjoining side roads of up to a factor of 5 can be observed. A total of 4.4% of the on-road measurements exceeded the WHO 1 h guideline value of  $200\ \mu\text{g m}^{-3} \approx 106\text{ ppb}$  (depending on temperature, here the appropriate conversion factor at  $25\text{ }^\circ\text{C}$  and 1013 hPa are used), corresponding to 4.1% of the area covered. Note that WHO reference concentration refers to 1 h average values, whereas we measure at each location for a few seconds. We use this comparison to show how often this threshold would be exceeded if the drive-by measurement were representative local respective situations. High  $\text{NO}_2$  values over motorways

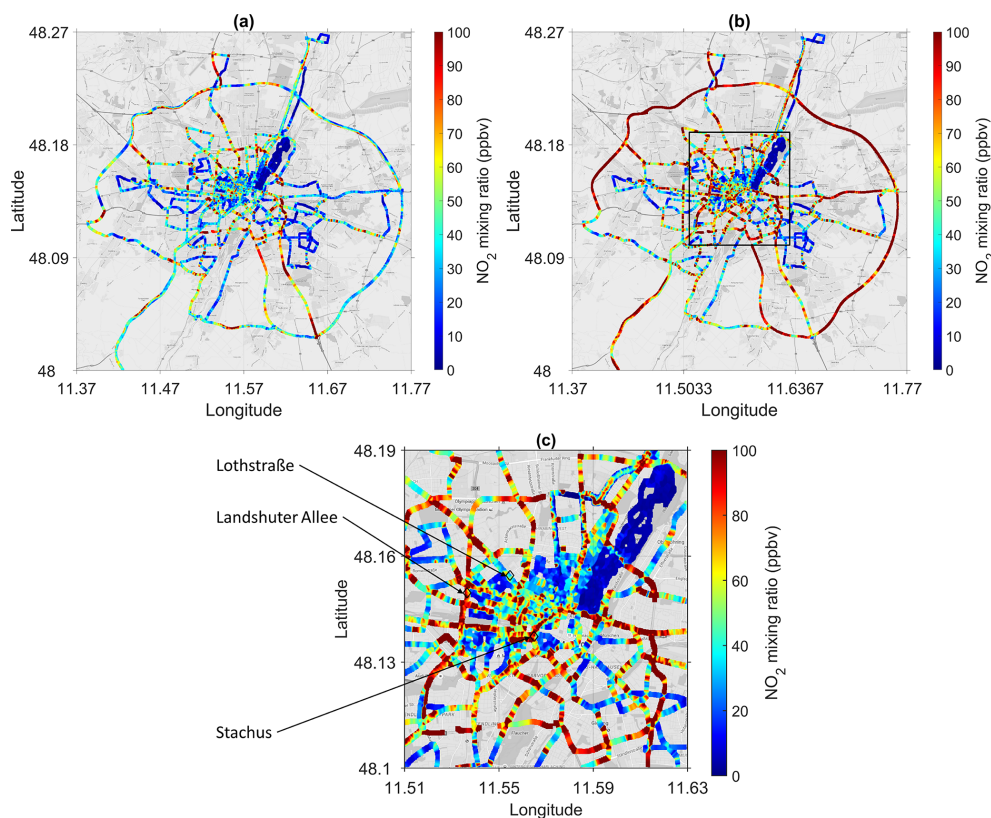


**Figure 4.** (a) CE DOAS and CAPS mobile measurements of NO<sub>2</sub> in Munich in 2016. (b) Normalized spatial distribution of NO<sub>2</sub> using coinciding LP DOAS data to remove the diurnal dependencies. (c) Close-up of the city center. The three black diamonds in panel (c) are the locations of the governmental monitoring stations (Landshuter Allee, Lothstraße, Stachus). The area at the top right with very low concentrations represents the city park English Garden. Map data © Google Maps.

**Table 2.** Percentage of measured concentrations exceeding the WHO AQG 1 h guideline and its corrected on-road level thresholds for both temporal and spatial coverage. The values are broken down for before and after the normalization of the data according to diurnal patterns and also calculated for WHO guideline values adjusted for the different measurement height and distance to the street.

	Percentage exceeding WHO guideline		Percentage exceeding adjusted WHO guideline	
	Before normalization	After normalization	Before normalization	After normalization
Temporally	4.4 %	14.5 %	1.7 %	6.7 %
Spatially (total)	4.1 %	17.1 %	1.1 %	4.6 %
Spatially (downtown)	5.5 %	12.4 %	1.6 %	4.7 %

were mainly due to the emission of heavy duty diesel vehicles; i.e., a significant increase could be observed when we were driving behind trucks and buses. In the city center traffic congestion and the street canyon effect (Rakowska et al., 2014) can be the main cause of elevated on-road NO<sub>2</sub> levels. Zhu et al. (2018) showed in a study in Hong Kong that average pollution exposure increases by 14.5 % when stopping at a traffic light compared to fluent traffic. Other studies showed as well that the distribution of pollutants is mainly impacted by traffic flow patterns (Fu et al., 2017; Rakowska et al., 2014; Huan and Kebin, 2012; Kaur et al., 2007; Westerdahl et al., 2005). The normalization using coinciding LP DOAS

measurement removes the diurnal dependency but leaves the traffic flow dependency in the data, because it contributes to the city-wide air quality. The normalized on-road NO<sub>2</sub> map shown in Fig. 4b represents daily average values for all locations. After normalization, there exist some regions where NO<sub>2</sub> concentrations are consistently higher, while in other areas the normalized concentrations are lower than the original measurements. This behavior can be explained by the time of the day when the measurements were taken: when we measured during the rush hour, the measurements were higher, while the measurements during noon are lower than the daily average. The normalization procedure increased the

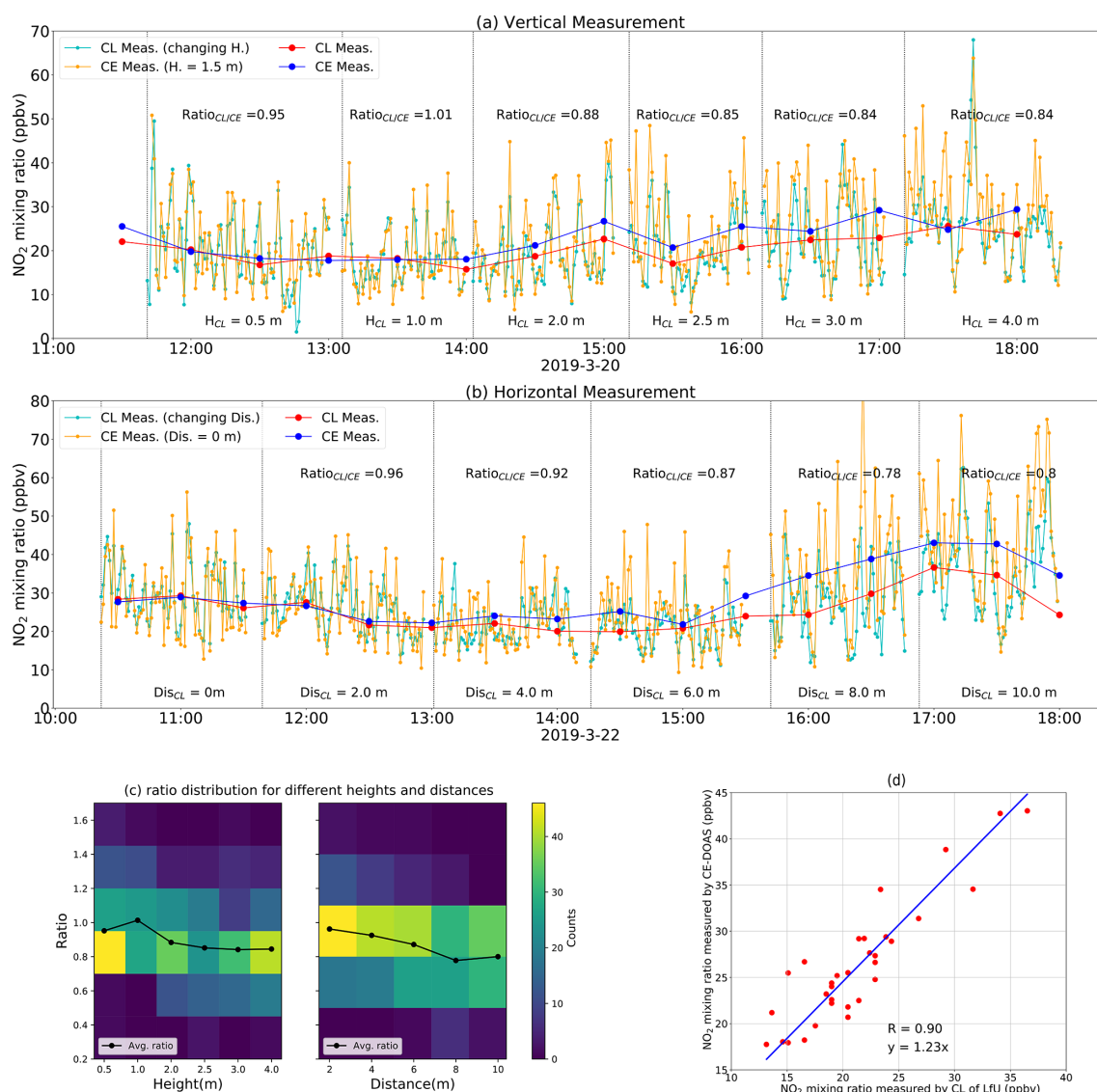


**Figure 5.**  $\text{NO}_2$  measurements at Karlsplatz (Stachus), Munich, with different heights above ground (a) and distances to the main street (b). The ratio between 1 min averaged CE DOAS and coinciding CL measurements were calculated individually for the different heights and distances. Half-hour averaged CE DOAS measurements (blue curve) were compared with the corresponding CL measurements (red curve). Averaged ratios for different heights and distances (as defined in panel a) are shown in panel (c); CE DOAS measurements at 1.5 m were averaged to 30 min intervals and compared with the half-hourly data of the governmental monitoring station at 4 m shown in panel (d).

occurrences of WHO 1 h guideline exceedances to 14.5 % of the on-road measurements, corresponding to 17.1 % of the total area (including motorways) and 15.7 % of the area in the city center. However, the thresholds in WHO AQG are based on studies involving monitoring station data which are not measuring directly on the street. Taking the vertical and horizontal dilution factors (see Fig. 5, the factor 0.84 for 4 m height and 0.87 for 6 m distance) into account, we extrapolate the WHO AQG 1 h threshold value of  $200 \mu\text{g m}^{-3}$  to the on-road level with the value of  $273.7 \mu\text{g m}^{-3} \approx 145.6 \text{ ppb}$  ( $200 \mu\text{g m}^{-3}/0.84/0.87$ ), and we then also calculated the frequency of exceedances (see Table 2).

It can be seen that, especially in the downtown area (Fig. 4c), the values after the normalization are noticeably higher than before. This can be explained as we tried to avoid the rush hours, i.e., traffic jams, for performing the measurements. Therefore, the measured  $\text{NO}_2$  level is often lower in comparison to the day average. The area with significantly lower concentrations seen in Fig. 4 is the city park (English Garden) with no vehicle emissions and where plants could provide deposition areas for  $\text{O}_3$ ,  $\text{NO}_x$  and particles (Chaparro-Suarez et al., 2011; Wesely and Hicks, 2000).

### 3.2 Comparison of NO<sub>2</sub> concentrations at different heights and distances from the street

In order to investigate the diffusion effects of emitted NO<sub>2</sub> molecules in both vertical and horizontal directions, measurements were conducted over two days (20 and 22 March 2019) using CE DOAS and CL instruments at Stachus, Munich, next to the governmental monitoring station. Since we used two different measurement techniques, the first step was to check the instrument for consistency. Side-by-side measurements next to the street (same height and distance to the street in Fig. 5) were used to analyze differences. We found the CL NO<sub>2</sub> to be 2 % higher, possibly due to sensitivities of the molybdenum oxide converters to NO<sub>y</sub> species (see Villena et al., 2012; Dunlea et al., 2007). We corrected the CL measurement data in order to remove those interferences.

Both instruments were set up next to the governmental monitoring station at Stachus, which is at a height of 4 m and has a 30 min time resolution. The CE DOAS was set up next to the street and measured at a fixed height of 1.5 m above the ground, while the CL instrument measured NO<sub>2</sub> at multiple heights above the ground (from 0.5 to 4 m) and at different distances from the side of the street (from 2 to 10 m). The temporal resolution for both instruments was set to 5 s. All measurements are shown in Fig. 5a for the different measurement heights and Fig. 5b for the different distances to the side of the street. Figure 5c shows the distribution of the ratios, and it can clearly be seen that the average concentrations decrease with height and distance. Another mobile measurement study by Apte et al. (2017) also demonstrates the distance-decay characteristic of the urban spatial distribution of NO, NO<sub>2</sub> and black carbon but on larger scales. More relevant theoretical decay research can be found in Choi et al. (2012, 2014). Figure 5d shows a two-day comparison between the 30 min average NO<sub>2</sub> concentrations measured with our CE DOAS at a height of 1.5 m with the CL instrument data of the governmental monitoring station at a height of 4 m. The regression plot shows a ratio of 1.23 between the measurements at 1.5 and 4 m height. In addition, the side-by-side measurement derives a factor of 0.84 with a standard deviation of 0.20, so most ratios vary from 37 % decrease with increasing height (factor  $0.84 - 0.20 = 0.64$ ) to 5 % increase (factor  $0.84 + 0.20 = 1.04$ ). Additional roadside measurements regarding the comparison between the 1.5 and 4 m measurement height were conducted at roadside next to the MIM building and the LfU station of Landshuter Allee on several different days during different seasons and derived a similar result. Since the inlet height for our mobile measurements is 1.5 m, we take this factor into account when comparing to monitoring station data. In addition, we analyzed how the uncertainty of the scaling factors (horizontal and vertical) contributes to the comparison with the WHO threshold shown in Table 2 and found that the percentage of exceedances can vary between 0.4 % and 23.8 %. It is be-

cause those dilution factors could vary, as they depend on factors in a small-scale environment, such as local meteorology, seasonality, local topography, urban morphology and traffic conditions. We do not assume that the scaling factors can be applied to all our mobile measurements but rather on average for our statistical analysis. For further distance-decay studies, it is essential to carry out more extensive and long-term side-by-side measurements to cover different measurement environments (such as different locations and seasons). In terms of distance to the street, measuring at the center of the street, like we did during the mobile measurements, and measuring at a distance of 6 m, which is approximately the distance of most monitoring stations to the middle of the street, the on-road measurements are 13 % higher with a standard deviation of 0.18 due to the observed diffusion effects. Those factors have to be kept in mind when comparing on-road measurements to monitoring station data or any other measurement data taken at different height levels and distances to the street. This leads to the conclusion that from the 48 % difference between the average concentrations of three monitoring stations ( $48 \mu\text{g m}^{-3}$ ) and the mobile measurements around the three stations ( $93 \mu\text{g m}^{-3}$ ), both averaged for the measurement campaign period, 27 % can be explained by the difference in inlet height and distance to the street, and the remaining 21 % is due to the fact that the monitoring stations are positioned away from pollution hot spots at crossroads according to WHO guidelines.

## 4 Summary and conclusions

Mobile road measurements using CE DOAS and CAPS instruments combined with an algorithm for correcting the diurnal cycle were used in order to generate a consistent pollution map of the street level NO<sub>2</sub> concentration in Munich. This map is not only used to identify pollution hot spots but also to figure out how representative the existing NO<sub>2</sub> point measurements are for the whole city. Elevated NO<sub>2</sub> levels can be observed mostly on motorways and busy city roads, due to the emission of heavy duty vehicles or heavy traffic volume. When averaging the mobile measurements around the monitoring stations, we derived an average NO<sub>2</sub> concentration of  $93 \mu\text{g m}^{-3}$ , whereas the three monitoring stations at the city center reported  $48 \mu\text{g m}^{-3}$  on average for the same time, so 48 % lower values. Our analysis shows that the different measurement height can account for 16 % difference (factor 0.84), and the distance of the sample inlets to the center of the street, where the mobile measurements took place, explains the 13 % (factor 0.87) lower values. Accounting for these factors still leaves about 21 % that can be attributed to pollution hot spots like busy crossroads or tunnel exits. These hot spots are not covered by monitoring stations, which is intentionally done in order to make the long-term data less dependent on local events. Nevertheless, the differences observed in the presented study show that point measurements



are likely not representative for the NO<sub>2</sub> concentration in the whole city. Most network measurement sites are not capturing the concentrations people are exposed to when walking or driving at the street level but are instead focusing on long-term trends. Our study illustrates the importance of combining different measurement techniques to capture spatial and temporal patterns within a city and derive concentration values that are representative for the air most people breathe in.

The pollution maps generated in this project provide valuable information for future urban planning and the design of control measures of environment pollution. Furthermore, it can provide guidelines for identifying representative locations for air pollution monitoring stations in a city. Additionally, the observed spatial distribution of NO<sub>2</sub> concentrations is also beneficial to the validation of chemical transport models and assessment studies of the impact of air pollution on human health.

*Data availability.* The data that support the findings of this study are available on request from the corresponding author Ying Zhu and Mark Wenig. The data are not publicly available due to them containing information that could compromise research participant consent.

*Supplement.* The supplement related to this article is available online at: <https://doi.org/10.5194/acp-20-13241-2020-supplement>.

*Author contributions.* YZ, MW and JC designed the experiments. YZ, GK and XB carried them out. KLC simulated the results from the GEOS-Chem model. YZ prepared the manuscript with contributions from all coauthors.

*Competing interests.* The authors declare that they have no conflict of interest.

*Acknowledgements.* The work described in this paper was jointly supported by the major research instrumentation program INST 86/1499 FUGG. In addition, Ying Zhu, Jia Chen, Xiao Bi, and Florian Dietrich was partly funded by the Deutsche Forschungsgemeinschaft (DFG, German Research Foundation) – CH 1792/2-1 and supported by Technical University of Munich – Institute for Advanced Study, funded by the German Excellence Initiative and the European Union Seventh Framework Program under grant agreement number 291763.

*Financial support.* This work was supported by the German Research Foundation (DFG) and the Technical University of Munich (TUM) in the framework of the Open Access Publishing Program.

*Review statement.* This paper was edited by Ronald Cohen and reviewed by three anonymous referees.

## References

- Apte, J. S., Messier, K. P., Gani, S., Brauer, M., Kirchstetter, T. W., Lunden, M. M., Marshall, J. D., Portier, C. J., Vermeulen, R. C., and Hamburg, S. P.: High-resolution air pollution mapping with Google street view cars: exploiting big data, *Environ. Sci. Technol.*, 51, 6999–7008, 2017.
- Ball, S. M. and Jones, R. L.: Broad-band cavity ring-down spectroscopy, *Chem. Rev.*, 103, 5239–5262, 2003.
- Ban-Weiss, G. A., McLaughlin, J. P., Harley, R. A., Lunden, M. M., Kirchstetter, T. W., Kean, A. J., Strawa, A. W., Stevenson, E. D., and Kendall, G. R.: Long-term changes in emissions of nitrogen oxides and particulate matter from on-road gasoline and diesel vehicles, *Atmos. Environ.*, 42, 220–232, 2008.
- Berden, G., Peeters, R., and Meijer, G.: Cavity ring-down spectroscopy: Experimental schemes and applications, *Int. Rev. Phys. Chem.*, 19, 565–607, 2000.
- Brown, S., Stark, H., and Ravishankara, A.: Cavity ring-down spectroscopy for atmospheric trace gas detection: application to the nitrate radical (NO<sub>3</sub>), *Appl. Phys. B*, 75, 173–182, 2002.
- Chan, K. L., Wang, S., Liu, C., Zhou, B., Wenig, M. O., and Saiz-Lopez, A.: On the summertime air quality and related photochemical processes in the megacity Shanghai, China, *Sci. Total Environ.*, 580, 974–983, <https://doi.org/10.1016/j.scitotenv.2016.12.052>, 2017.
- Chaparro-Suarez, I., Meixner, F., and Kesselmeier, J.: Nitrogen dioxide (NO<sub>2</sub>) uptake by vegetation controlled by atmospheric concentrations and plant stomatal aperture, *Atmos. Environ.*, 45, 5742–5750, <https://doi.org/10.1016/j.atmosenv.2011.07.021>, 2011.
- Choi, W., He, M., Barbesant, V., Kozawa, K. H., Mara, S., Winer, A. M., and Paulson, S. E.: Prevalence of wide area impacts downwind of freeways under pre-sunrise stable atmospheric conditions, *Atmos. Environ.*, 62, 318–327, 2012.
- Choi, W., Winer, A. M., and Paulson, S. E.: Factors controlling pollutant plume length downwind of major roadways in nocturnal surface inversions, *Atmos. Chem. Phys.*, 14, 6925–6940, <https://doi.org/10.5194/acp-14-6925-2014>, 2014.
- Commission, E.: Directive 2008/50/EC of the European Parliament and of the Council of 21 May 2008 on ambient air quality and cleaner air for Europe, *Official Journal of the European Union*, 19 pp., 2008.
- Dunlea, E. J., Herndon, S. C., Nelson, D. D., Volkamer, R. M., San Martini, F., Sheehy, P. M., Zahniser, M. S., Shorter, J. H., Wormhoudt, J. C., Lamb, B. K., Allwine, E. J., Gaffney, J. S., Marley, N. A., Grutter, M., Marquez, C., Blanco, S., Cardenas, B., Retama, A., Ramos Villegas, C. R., Kolb, C. E., Molina, L. T., and Molina, M. J.: Evaluation of nitrogen dioxide chemiluminescence monitors in a polluted urban environment, *Atmos. Chem. Phys.*, 7, 2691–2704, <https://doi.org/10.5194/acp-7-2691-2007>, 2007.
- EEA: Air quality in Europe–2017 Report, *Tech. Rep.*, European Environment Agency Copenhagen, Denmark, 41–42, 2017.
- Engeln, R., von Helden, G., Berden, G., and Meijer, G.: Phase shift cavity ring down absorption spectroscopy, *Chem. Phys. Lett.*,

- 262, 105–109, [https://doi.org/10.1016/0009-2614\(96\)01048-2](https://doi.org/10.1016/0009-2614(96)01048-2), 1996.
- Fu, X., Liu, J., Ban-Weiss, G. A., Zhang, J., Huang, X., Ouyang, B., Popoola, O., and Tao, S.: Effects of canyon geometry on the distribution of traffic-related air pollution in a large urban area: Implications of a multi-canyon air pollution dispersion model, *Atmos. Environ.*, 165, 111–121, <https://doi.org/10.1016/j.atmosenv.2017.06.031>, 2017.
- Ge, B., Sun, Y., Liu, Y., Dong, H., Ji, D., Jiang, Q., Li, J., and Wang, Z.: Nitrogen dioxide measurement by cavity attenuated phase shift spectroscopy (CAPS) and implications in ozone production efficiency and nitrate formation in Beijing, China, *J. Geophys. Res.-Atmos.*, 118, 9499–9509, 2013.
- Henderson, S. B., Beckerman, B., Jerrett, M., and Brauer, M.: Application of land use regression to estimate long-term concentrations of traffic-related nitrogen oxides and fine particulate matter, *Environ. Sci. Technol.*, 41, 2422–2428, 2007.
- Herbelin, J. M., McKay, J. A., Kwok, M. A., Ueunten, R. H., Urevig, D. S., Spencer, D. J., and Benard, D. J.: Sensitive measurement of photon lifetime and true reflectances in an optical cavity by a phase-shift method, *Appl. Opt.*, 19, 144–147, <https://doi.org/10.1364/AO.19.000144>, 1980.
- Hermans, C., Vandaele, A. C., Carleer, M., Fally, S., Colin, R., Jenouvrier, A., Coquart, B., and Mérienne, M.-F.: Absorption cross-sections of atmospheric constituents: NO<sub>2</sub>, O<sub>2</sub>, and H<sub>2</sub>O, *Environ. Sci. Pollut. Res.*, 6, 151–158, <https://doi.org/10.1007/BF02987620>, 1999.
- Huan, L. and Kebin, H.: Traffic Optimization: A New Way for Air Pollution Control in China's Urban Areas, *Environ. Sci. Technol.*, 46, 5660–5661, <https://doi.org/10.1021/es301778b>, 2012.
- Huang, R.-J., Zhang, Y., Bozzetti, C., Ho, K.-F., Cao, J.-J., Han, Y., Daellenbach, K. R., Slowik, J. G., Platt, S. M., Canonaco, F., Zotter, P., Wolf, R., Pieber, S. M., Brun, E. A., Crippa, M., Ciarelli, G., Piazzalunga, A., Schwikowski, M., Abbaszade, G., Schnelle-Kreis, J., Zimmermann, R., An, Z., Szidat, S., Baltensperger, U., Haddad, I. E., and Prévôt, A. S. H.: High secondary aerosol contribution to particulate pollution during haze events in China, *Nature*, 514, 218–222, 2014.
- Jang, M. and Kamens, R. M.: Characterization of Secondary Aerosol from the Photooxidation of Toluene in the Presence of NO<sub>x</sub> and 1-Propene, *Environ. Sci. Technol.*, 35, 3626–3639, <https://doi.org/10.1021/es010676+>, 2001.
- Kaur, S., Nieuwenhuijsen, M., and Colville, R.: Fine particulate matter and carbon monoxide exposure concentrations in urban street transport microenvironments, *Atmos. Environ.*, 41, 4781–4810, <https://doi.org/10.1016/j.atmosenv.2007.02.002>, 2007.
- Kebabian, P. L., Herndon, S. C., and Freedman, A.: Detection of Nitrogen Dioxide by Cavity Attenuated Phase Shift Spectroscopy, *Anal. Chem.*, 77, 724–728, <https://doi.org/10.1021/ac048715y>, 2005a.
- Kebabian, P. L., Herndon, S. C., and Freedman, A.: Detection of nitrogen dioxide by cavity attenuated phase shift spectroscopy, *Anal. Chem.*, 77, 724–728, 2005b.
- Kebabian, P. L., Wood, E. C., Herndon, S. C., and Freedman, A.: A practical alternative to chemiluminescence-based detection of nitrogen dioxide: Cavity attenuated phase shift spectroscopy, *Environ. Sci. Technol.*, 42, 6040–6045, 2008.
- Kirchstetter, T. W., Harley, R. A., Kreisberg, N. M., Stolzenburg, M. R., and Hering, S. V.: On-road measurement of fine particle and nitrogen oxide emissions from light-and heavy-duty motor vehicles, *Atmos. Environ.*, 33, 2955–2968, 1999.
- Kraus, S.: DOASIS A Framework Design for DOAS, Ph.D. thesis, Combined Faculties for Mathematics and for Computer Science, University of Mannheim, 2005.
- Kundu, S., Deming, B. L., Lew, M. M., Bottorff, B. P., Rickly, P., Stevens, P. S., Dusanter, S., Sklaveniti, S., Leonardis, T., Locoge, N., and Wood, E. C.: Peroxy radical measurements by ethane – nitric oxide chemical amplification and laser-induced fluorescence during the IRRONIC field campaign in a forest in Indiana, *Atmos. Chem. Phys.*, 19, 9563–9579, <https://doi.org/10.5194/acp-19-9563-2019>, 2019.
- Langridge, J. M., Ball, S. M., and Jones, R. L.: A compact broadband cavity enhanced absorption spectrometer for detection of atmospheric NO<sub>2</sub> using light emitting diodes, *Analyst*, 131, 916–922, 2006.
- LfU: Untersuchung der räumlichen Verteilung der NO<sub>x</sub>-Belastung im Umfeld von vorhandenen, hochbelasteten Luftmessstationen, Abschlussbericht, Tech. Rep., Bayerisches Landesamt für Umwelt, 16–23, 2015.
- LfU, B.: Aktuelle Werte der bayerischen Luftmessstationen, available at: <https://www.lfu.bayern.de/luft/immissionsmessungen/messwerte/index.htm>, last access: 29 November 2019.
- Massman, W.: A review of the molecular diffusivities of H<sub>2</sub>O, CO<sub>2</sub>, CH<sub>4</sub>, CO, O<sub>3</sub>, SO<sub>2</sub>, NH<sub>3</sub>, N<sub>2</sub>O, NO, and NO<sub>2</sub> in air, O<sub>2</sub> and N<sub>2</sub> near STP, *Atmos. Environ.*, 32, 1111–1127, 1998.
- Min, K.-E., Washenfelder, R. A., Dubé, W. P., Langford, A. O., Edwards, P. M., Zarzana, K. J., Stutz, J., Lu, K., Rohrer, F., Zhang, Y., and Brown, S. S.: A broadband cavity enhanced absorption spectrometer for aircraft measurements of glyoxal, methylglyoxal, nitrous acid, nitrogen dioxide, and water vapor, *Atmos. Meas. Tech.*, 9, 423–440, <https://doi.org/10.5194/amt-9-423-2016>, 2016.
- Ning, Z., Wubulihai, M., and Yang, F.: PM, NO<sub>x</sub> and butane emissions from on-road vehicle fleets in Hong Kong and their implications on emission control policy, *Atmos. Environ.*, 61, 265–274, <https://doi.org/10.1016/j.atmosenv.2012.07.047>, 2012.
- Platt, U., Meinen, J., Pöhler, D., and Leisner, T.: Broadband Cavity Enhanced Differential Optical Absorption Spectroscopy (CE-DOAS) – applicability and corrections, *Atmos. Meas. Tech.*, 2, 713–723, <https://doi.org/10.5194/amt-2-713-2009>, 2009.
- Rakowska, A., Wong, K. C., Townsend, T., Chan, K. L., Westerdaal, D., Ng, S., Močnik, G., Drinovec, L., and Ning, Z.: Impact of traffic volume and composition on the air quality and pedestrian exposure in urban street canyon, *Atmos. Environ.*, 98, 260–270, <https://doi.org/10.1016/j.atmosenv.2014.08.073>, 2014.
- Rothman, L., Barbe, A., Benner, D. C., Brown, L., Camy-Peyret, C., Carleer, M., Chance, K., Clerbaux, C., Dana, V., Devi, V., Fayt, A., Flaud, J.-M., Gamache, R., Goldman, A., Jacquemart, D., Jucks, K., Lafferty, W., Mandin, J.-Y., Massie, S., Nemtchinov, V., Newnham, D., Perrin, A., Rinsland, C., Schroeder, J., Smith, K., Smith, M., Tang, K., Toth, R., Auwera, J. V., Varanasi, P., and Yoshino, K.: The HITRAN molecular spectroscopic database: edition of 2000 including updates through 2001, *J. Quant. Spectrosc. Ra.*, 82, 5–44, [https://doi.org/10.1016/S0022-4073\(03\)00146-8](https://doi.org/10.1016/S0022-4073(03)00146-8), 2003.
- Thalman, R. and Volkamer, R.: Inherent calibration of a blue LED-CE-DOAS instrument to measure iodine oxide, glyoxal, methyl glyoxal, nitrogen dioxide, water vapour and aerosol ex-

- inction in open cavity mode, *Atmos. Meas. Tech.*, 3, 1797–1814, <https://doi.org/10.5194/amt-3-1797-2010>, 2010.
- UBA: Air quality 2016 (Preliminary Evaluation), Tech. rep., Umweltbundesamt (German Environment Agency), 2017.
- Uhrner, U., von Löwis, S., Vehkamäki, H., Wehner, B., Bräsel, S., Hermann, M., Stratmann, F., Kulmala, M., and Wiedensohler, A.: Dilution and aerosol dynamics within a diesel car exhaust plume-CFD simulations of on-road measurement conditions, *Atmos. Environ.*, 41, 7440–7461, <https://doi.org/10.1016/j.atmosenv.2007.05.057>, 2007.
- Vandaele, A. C., Hermans, C., Fally, S., Carleer, M., Colin, R., Mérienne, M.-F., Jenouvrier, A., and Coquart, B.: High-resolution Fourier transform measurement of the NO<sub>2</sub> visible and near-infrared absorption cross sections: Temperature and pressure effects, *J. Geophys. Res.-Atmos.*, 107, 4348, <https://doi.org/10.1029/2001JD000971>, 2002.
- Venables, D. S., Gherman, T., Orphal, J., Wenger, J. C., and Ruth, A. A.: High sensitivity in situ monitoring of NO<sub>3</sub> in an atmospheric simulation chamber using incoherent broadband cavity-enhanced absorption spectroscopy, *Environ. Sci. Technol.*, 40, 6758–6763, 2006.
- Villena, G., Bejan, I., Kurtenbach, R., Wiesen, P., and Kleffmann, J.: Interferences of commercial NO<sub>2</sub> instruments in the urban atmosphere and in a smog chamber, *Atmos. Meas. Tech.*, 5, 149–159, <https://doi.org/10.5194/amt-5-149-2012>, 2012.
- Vogt, R., Scheer, V., Casati, R., and Benter, T.: On-Road Measurement of Particle Emission in the Exhaust Plume of a Diesel Passenger Car, *Environ. Sci. Technol.*, 37, 4070–4076, <https://doi.org/10.1021/es0300315>, 2003.
- Volkamer, R., Spietz, P., Burrows, J., and Platt, U.: High-resolution absorption cross-section of glyoxal in the UV–VIS and IR spectral ranges, *J. Photoch. Photobio. A*, 172, 35–46, <https://doi.org/10.1016/j.jphotochem.2004.11.011>, 2005.
- Washenfelder, R. A., Langford, A. O., Fuchs, H., and Brown, S. S.: Measurement of glyoxal using an incoherent broadband cavity enhanced absorption spectrometer, *Atmos. Chem. Phys.*, 8, 7779–7793, <https://doi.org/10.5194/acp-8-7779-2008>, 2008.
- Wesely, M. and Hicks, B.: A review of the current status of knowledge on dry deposition, *Atmos. Environ.*, 34, 2261–2282, 2000.
- Westerdahl, D., Fruin, S., Sax, T., Fine, P. M., and Sioutas, C.: Mobile platform measurements of ultrafine particles and associated pollutant concentrations on freeways and residential streets in Los Angeles, *Atmos. Environ.*, 39, 3597–3610, <https://doi.org/10.1016/j.atmosenv.2005.02.034>, 2005.
- Xie, C., Xu, W., Wang, J., Wang, Q., Liu, D., Tang, G., Chen, P., Du, W., Zhao, J., Zhang, Y., Zhou, W., Han, T., Bian, Q., Li, J., Fu, P., Wang, Z., Ge, X., Allan, J., Coe, H., and Sun, Y.: Vertical characterization of aerosol optical properties and brown carbon in winter in urban Beijing, China, *Atmos. Chem. Phys.*, 19, 165–179, <https://doi.org/10.5194/acp-19-165-2019>, 2019.
- Xie, Y., Zhao, B., Zhang, L., and Luo, R.: Spatiotemporal variations of PM<sub>2.5</sub> and PM<sub>10</sub> concentrations between 31 Chinese cities and their relationships with SO<sub>2</sub>, NO<sub>2</sub>, CO and O<sub>3</sub>, *Particuology*, 20, 141–149, 2015.
- Yoo, J.-M., Lee, Y.-R., Kim, D., Jeong, M.-J., Stockwell, W. R., Kundu, P. K., Oh, S.-M., Shin, D.-B., and Lee, S.-J.: New indices for wet scavenging of air pollutants (O<sub>3</sub>, CO, NO<sub>2</sub>, SO<sub>2</sub>, and PM<sub>10</sub>) by summertime rain, *Atmos. Environ.*, 82, 226–237, 2014.
- Zhu, Y., Chan, K. L., Lam, Y. F., Horbanski, M., Pöhler, D., Boll, J., Lipkowitzsch, I., Ye, S., and Wenig, M.: Analysis of spatial and temporal patterns of on-road NO<sub>2</sub> concentrations in Hong Kong, *Atmos. Meas. Tech.*, 11, 6719–6734, <https://doi.org/10.5194/amt-11-6719-2018>, 2018.